Size-Tunable, Bright, and Stable PbS Quantum Dots: A Surface Chemistry Study

Iwan Moreels,[†,*] Yolanda Justo,[†] Bram De Geyter,[†] Katrien Haustraete,[‡] José C. Martins,[‡] and Zeger Hens[†,*]

[†]Physics and Chemistry of Nanostructures, Ghent University, Krijgslaan 281-S3, BE-9000 Gent, Belgium, and [‡]NMR and Structure Analysis Unit, Ghent University, Krijgslaan 281-S4bis, BE-9000 Gent, Belgium

ABSTRACT PbS Qdots are synthesized using $PbCl_2$ and elemental sulfur as precursors. The available size range is significantly expanded using tri-*n*-octylphosphine (TOP), enabling the synthesis of monodisperse suspensions of Qdots with a mean size varying between 3 and 10 nm. The ligand composition and dynamics are investigated with nuclear magnetic resonance (NMR) spectroscopy. We show that the Qdots are passivated solely by highly dynamic OlAm ligands, even when TOP is employed during synthesis. In this respect, TOP is a compound strongly modifying the Qdot synthesis, without affecting the final Qdot surface chemistry. Next, the OlAm ligands are exchanged for oleic acid (OlAc). NMR data show that the OlAc ligands are tightly bound to the Qdot surface, with a coverage of 3.0 ± 0.4 nm^{-2}. In addition, we demonstrate that they are bound as oleate ions. Combining this with the inorganic Qdot composition, we observe that charge-neutral Qdots are obtained when taking into account the charge of the stoichiometric PbS Qdot core, the surface excess of Pb ions, the surface-adsorbed Cl ions and the oleate ligands. The Qdot suspensions are stable under atmospheric conditions, showing no changes in the NMR and absorbance spectra for several weeks. Finally, we determine the photoluminescence quantum yield (PL QY) for OlAc-capped PbS Qdots, synthesized either with or without TOP. In both cases, they are highly luminescent, with PL QY values varying between 20 and 90%, depending on the Qdot size.

KEYWORDS: semiconductor nanocrystals · lead chalcogenide · nuclear magnetic resonance spectroscopy · luminescence spectroscopy

Colloidal lead chalcogenide quantum dots (Qdots) are an increasingly important class of nanosized materials. High-quality PbS,[1,2] PbSe,[3] and PbTe[4] can all be synthesized by wet chemistry techniques, which produce suspensions of monodisperse Qdots (relative size dispersion $\sigma_d < 10\%$). This enables low-cost wet processing of the Qdots, and consequently, a variety of devices are currently pursued. PbTe Qdots, for instance, offer prospects for enhanced thermoelectric properties, and substantial progress has been made toward the fabrication of highly conductive n- and p-type thin films.[5,6] Photonic applications involving lead chalcogenide Qdots are mostly based on PbS and PbSe: Qdot-based electroluminescent devices,[7,8] lasers,[9] solar cells,[10,11] and photodetectors[12,13] have all been demonstrated. In these fields, it is not yet clear whether PbS or PbSe Qdots are the more suitable. For instance, photodetectors are often PbS-based.[12,13] In contrast, early solar cell applications primarily used PbSe Qdots;[10] only recently Tang *et al.*[14] demonstrated that PbS Qdots offer an enhanced stability under ambient conditions, and Ma *et al.*[15] showed that solar cells consisting of PbS_xSe_{1-x} alloyed Qdots take advantage of both an improved open circuit voltage and short circuit photocurrent.

From an optical perspective, both the absorption and luminescence properties make the materials equally attractive for photonic devices. They show a similar molar extinction coefficient at the band gap,[16,17] and both materials have a high photoluminescence quantum yield (PL QY). Values for small PbSe Qdots vary between 12 and 85%,[18−20] while for PbS Qdots, a PL QY between 20 and 82% has been reported.[1,2,21−23] PbSe Qdots have, however, practical disadvantages: several studies have already reported on their poor stability in air.[24−26] This is a serious drawback if one wishes to operate PbSe-based devices under ambient atmosphere. In this respect, PbS Qdots may offer a suitable alternative to PbSe Qdots, and hence, a synthesis which produces a large size range of bright and stable PbS Qdots is higly desirable.

For PbS Qdots, currently two organic synthesis routes exist. The first route is based on lead oleate reacting with bis(trimethylsilyl)-sulfide in octadecene (referred to as the Hines synthesis from here on).[1] It offers monodisperse Qdots over a wide size range (2.6−7.2 nm, corresponding to an absorption peak of 825−1750 nm), and the Qdots are bright,[1,21−23] yet not entirely air-stable for all sizes.[27] The second route employs lead chloride ($PbCl_2$) and elemental sulfur (S) in oleylamine (OlAm) as precursors and OlAm as the solvent (Cademartiri synthesis).[2] The

* Address correspondence to iwan.moreels@ugent.be, zeger.hens@ugent.be.

Received for review November 10, 2010 and accepted February 15, 2011.

Published online February 28, 2011
10.1021/nn103050w

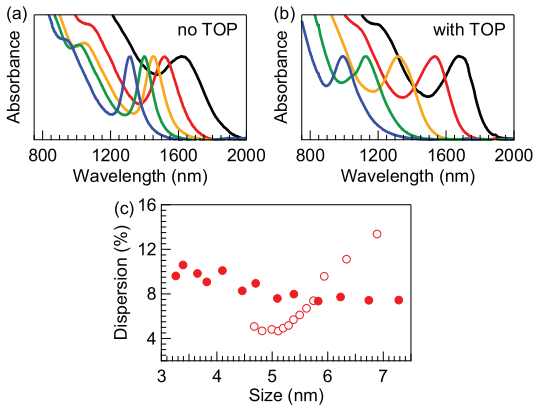

Figure 1. Series of absorbance spectra for PbS Qdots synthesized at 120 °C, without (a) and with (b) TOP added to the synthesis. Aliquots taken at 20 s (blue), 100 s (green), 450 s (yellow), 33 min (red), and 90 min (black) are shown. (c) Relative size dispersion σ_d of the aliquots for the TOP-less (○) and TOP-containing (●) synthesis.

TABLE 1. Syntheses Carried out at 120 °C, Using the Concentrations Indicated (in mol/L)

no.	$PbCl_2$	OlAm-S	TOPS
S1	0.4	0.1	0
S2	0.4	0.05	0.05
S3	0.4	0.05	0

available size range is substantially smaller (4.2−6.4 nm, corresponding to an absorption peak of 1200−1600 nm), yet the Qdots also have a high PL QY,[2] and thin films of these Qdots show good optical stability.[28]

In this paper, we further tune the Cademartiri synthesis to produce a wide size range of PbS Qdots with a high PL QY. To achieve size-tunability, tri-*n*-octylphosphine (TOP) is added. A pivotal element presented here is the characterization of the organic ligands using nuclear magnetic resonance (NMR) spectroscopy. Both the composition and adsorption/desorption dynamics of the ligand shell are studied, which reveal a peculiar role for TOP during synthesis. Next, the NMR results on the as-synthesized Qdots are used to rationalize a subsequent exchange to oleic acid (OlAc) ligands. The resulting Qdots have a PL QY of 20−90%, depending on size. In addition, PbS Qdots produced by our modified Cademartiri synthesis are air-stable over the entire size range studied, in contrast with larger PbS Qdots obtained by the Hines synthesis.[27]

RESULTS AND DISCUSSION

PbS Qdot Synthesis. Figure 1a shows absorbance spectra for a typical Cademartiri synthesis (Table 1, reaction S1). Previously published conclusions[2] are confirmed by our results: a strong nucleation event is followed by a limited Qdot growth, leading to monodisperse Qdot suspensions with a mean size ranging from 4.7 nm (after 20 s) to 5.5 nm (after 12 min,

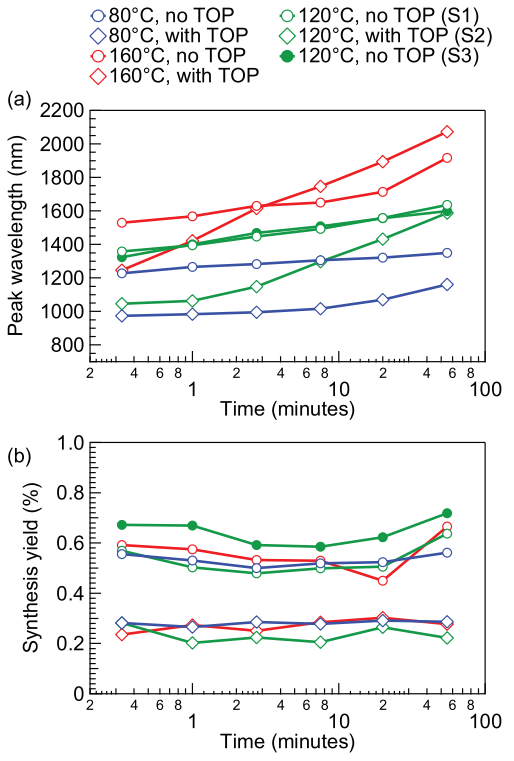

Figure 2. Spectral position of the Qdot first absorption peak as a function of time (log-scale) and temperature for syntheses with (◊) and without (○) TOP.

spectrum not shown). Hereafter, σ_d starts to increase strongly (Figure 1c, ○). To gain more insight into the reaction kinetics, we monitored the synthesis yield (*i.e.*, the fraction of S incorporated into the Qdots). Figure 2 (green ○) shows that the yield is constant throughout the synthesis, averaging 54% over the different aliquots taken. This remarkable result implies that, even after 20 s, the Qdots no longer grow by the incorporation of additional monomers (the reaction scheme most often encountered in colloidal quantum dot synthesis).[29,30] At this stage, the synthesis must then be based on a ripening mechanism, either involving the growth of bigger particles at the expense of smaller ones (Ostwald ripening) or involving a coalescence of Qdots.[31]

As a result, the Cademartiri synthesis only offers a limited range for which monodisperse Qdot suspensions can be obtained, and varying the temperature (Figure 2a, ○) between 80 and 160 °C does not substantially increase it. To overcome this drawback, we introduce TOPS as a low-reactivity S precursor. The rationale is that a precursor with a low but nonzero reactivity could lead to prolonged Qdot growth after the nucleation of PbS from $PbCl_2$ and OlAm-S. Hence, larger Qdots should be obtainable without a strong increase in size dispersion, similar to a secondary injection of precursors.[32] Figure 1b shows absorbance spectra of a series of aliquots for PbS Qdots synthesized at 120 °C, with 170 μL of TOP added to the synthesis

(Table 1, reaction S2, TOPS/OlAm-S ratio of 1:1). As anticipated, the transformation of 50% of OlAm-S to TOPS appears to extend the Qdot growth. For comparison, after 20 s, we obtain 3.3 nm Qdots, which grow up to 5.1 nm after 12 min and finally 7.3 nm after 2.5 h. The synthesis yield drops to 23% (Figure 2b, green ◊), again being constant as a function of time. At both higher and lower temperatures, a similar result is obtained (Figure 2b, ◊). Although the reduced yield confirms that the addition of TOPS leads to fewer nuclei being formed (*i.e.*, TOPS is not included during nucleation), its time independence again hints toward a more complex reaction mechanism based on ripening. Possibly, the major role of TOPS is merely to facilitate this ripening, as the enhanced growth rate and constant yield suggests. Note that monodispersity is maintained in reaction S2 (Figure 1c, ●). For Qdots larger than *ca.* 6 nm, this leads to an improved σ_d compared to the TOP-less synthesis (a similar behavior is observed at other temperatures). Although uncommon for ripening-based reactions, this has already been observed in literature, both in the case of Ostwald ripening[2,33] and Qdot coalescence.[31] Hence, ripening does not necessarily lead to an increase in σ_d.

The heterogeneous synthesis described here is presently not yet fully understood. In addition, similar to the case of PbSe Qdots synthesized from lead oleate and TOPSe, impurities in TOP may influence the results.[34] However, despite the need for further experimental data and theoretical modeling of this reaction, the observation that TOPS is not a mere stable, unreactive compound present during synthesis is clearly verified by a control experiment. When simply reducing the OlAm-S concentration by 50%, without addition of TOPS (Table 1, reaction S3), we do not observe any changes in the Qdot growth kinetics compared to reaction S1, apart from a slight increase of the yield to 63% (Figure 2, ●).

Using growth temperatures from 80 to 160 °C, replacement of 50% of OlAm-S by TOPS consistently leads to a wider range of sizes accessible (Figure 2a, ◊). As a result, Qdots between 3 and 10 nm can now be synthesized *via* a one-step procedure, spanning a range of band gaps going from 1.34 eV (925 nm) down to 0.59 eV (2100 nm). In Figure 3, we display the optimal results. Full lines represent Qdots synthesized using TOP; the larger sizes typically have a better σ_d when prepared with TOP, while Qdots with a peak absorption below 1200 nm cannot be obtained without it. For Qdots with a exciton peak between 1200 and 1600 nm, the original Cademartiri synthesis still provides the best results (dotted lines). Note that in some cases we also observe large clusters in our suspension (Figure 3b). When this occurs, we simply remove these by size-selective precipitation, adding a small amount of ethanol (EtOH) to a suspension of PbS Qdots until precipitation starts. Figure 3c indeed shows that they can be efficiently removed.

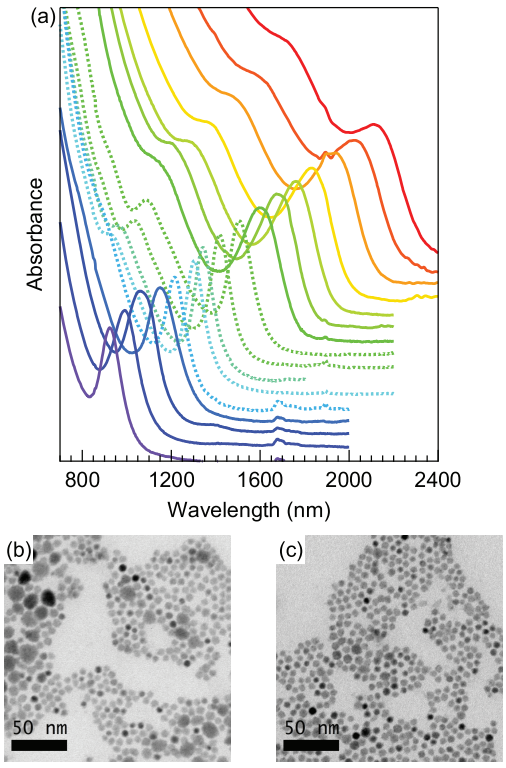

Figure 3. (a) Typical absorbance spectra of PbS Qdot suspensions. Full lines are Qdots synthesized with TOP, dotted lines without TOP. (b,c) TEM images of a typical PbS Qdot suspension before (b) and after (c) size-selective precipitation.

Ligand Identification. Particle stability in suspension and optical properties such as the Qdot luminescence heavily depend on the ligands attached to the surface. In this respect, it is important to understand the Qdot ligand composition and dynamics in order to optimize these properties. Given the strong influence of TOP on the Qdot synthesis, we focus on both OlAm and TOP as possible ligands. Importantly, amines are known to bind relatively weakly to the Qdot surface, resulting in highly dynamic ligands.[35−39] Indeed, as-synthesized PbS Qdots can only be precipitated and resuspended once, which already indicates a facile loss of ligands during particle processing.

We use solution NMR for the investigation of the Qdot ligands. It provides powerful techniques for a direct *in situ* view.[24,39−41] We first investigate PbS Qdots prepared without TOP. Figure 4a shows a typical proton (^{1}H) NMR spectrum of such Qdots (5.7 nm), suspended in deuterated toluene (tol-d_8, bottom). The spectrum compares well with a spectrum of OlAm dissolved in tol-d_8 (top), and the proton−carbon heteronuclear single quantum correlation (^{1}H−^{13}C HSQC) spectrum confirms that the PbS Qdot resonances indeed arise from OlAm (Figure 4b). However, in contrast with previous results on TOPO-capped InP[40] and OlAc-capped PbSe Qdots,[24] all except the resonance at 2.53 ppm show only a moderate

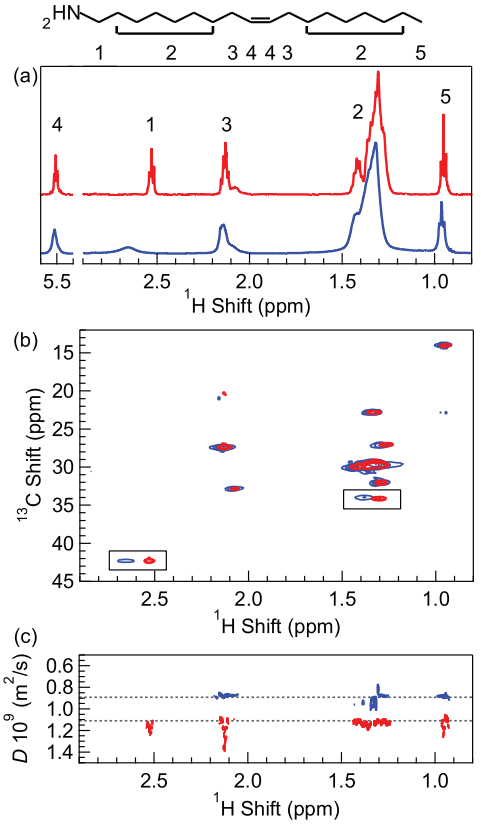

Figure 4. (a) ^{1}H NMR spectra of OlAm (top) and a PbS Qdot suspension (bottom) dissolved in tol-d_8. (b) HSQC spectra of OlAm (red) and a PbS Qdot suspension (blue). Except for the resonances at 2.53 and 1.42 ppm (boxes), we observe no significant downfield shift. (c) We observe a single diffusion coefficient in the DOSY spectrum of PbS Qdots (blue), 20% smaller than the value for free OlAm (red).

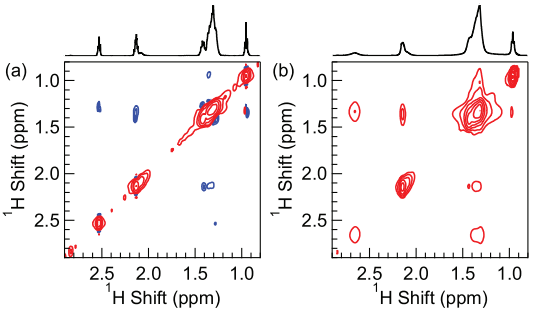

Figure 5. NOESY spectra of OlAm (a) and a PbS Qdot suspension (b) in tol-d_8. Cross-peaks indicating positive, respectively, negative NOEs have opposite (blue), respectively, the same (red) sign as the diagonal peaks (red). Positive NOE cross-peaks appear for free OlAm, while the dynamic OlAm ligands show negative NOE cross-peaks (red).

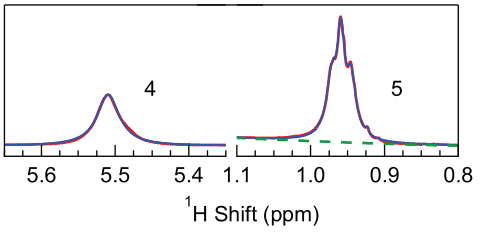

Figure 6. Quantitative ^{1}H NMR spectrum of PbS Qdots prepared with TOP. We fit the areas of the alkene (4) and methyl (5) protons by a sum of Lorentzian peaks, superimposed on a background in the case of the methyl protons (dashed line) to accommodate for the contribution of the neighboring CH_2 resonance.

broadening compared to the free OlAm resonances, and while we observe a downfield shift for the 2.53 and 1.42 ppm resonances (corresponding to the protons closest to the NH_2 headgroup), the other resonances do not reveal a significant shift. In addition, the PbS Qdot diffusion ordered spectroscopy (DOSY) data (measured with a gradient pulse duration δ = 3 ms and diffusion delay Δ = 125 ms, Figure 4c, blue) show a single value for the OlAm diffusion coefficient ($D = 8.9 \times 10^{-10}$ m^2/s), only reduced by 20% with respect to free OlAm ($D = 11.1 \times 10^{-10}$ m^2/s, red).

Consequently, the ^{1}H NMR and DOSY do not unambiguously show that OlAm is bound to the Qdot surface. To confirm that OlAm indeed acts as a ligand, nuclear Overhauser effect spectroscopy (NOESY) is performed. Figure 5 shows NOESY spectra for free OlAm and a PbS Qdot suspension, measured with a mixing time of 600 ms (free OlAm) and 100 ms (PbS Qdots), respectively. Free OlAm is a small molecule with an expected rotational correlation time smaller than the reciprocal of the spectrometer frequency (500 MHz). Hence, cross-peaks indicative of positive NOEs are observed (Figure 5a).[42] In contrast, the NOESY spectrum of the PbS Qdot suspension shows cross-peaks associated with negative NOEs (Figure 5b). These arise from a reduced rotational correlation time,[42] which we attribute to the interaction of OlAm with the large and slowly tumbling Qdots. Hence, the combined ^{1}H NMR, DOSY, and NOESY measurements lead to the conclusion that OlAm is a ligand in fast exchange between a free and a bound state. The exchange rate limit R is estimated from the chemical shift difference[43] of the α-CH_2 group (marked by 1 in Figure 4), which yields

$$R \gg \pi \nu_{TMS}(\delta_b - \delta_f) = 200\ s^{-1} \qquad (1)$$

δ_f and δ_b equal the chemical shift of the free and bound OlAm, respectively; ν_{TMS} is the frequency of the reference compound tetramethylsilane, equal to 500.13 MHz.

For PbS Qdots synthesized in the presence of TOP, we again observe the OlAm resonances in the ^{1}H NMR spectrum. Details of a typical spectrum of such Qdots (5.7 nm) are shown in Figure 6. To calculate the amount of TOP, we use quantitative ^{1}H NMR. We determine the composition of the ligand shell as follows: both TOP and OlAm can contribute to the methyl resonance, while only OlAm will contribute to the alkene resonance. Hence, taking the corresponding number of protons into account, the methyl−alkene area ratio

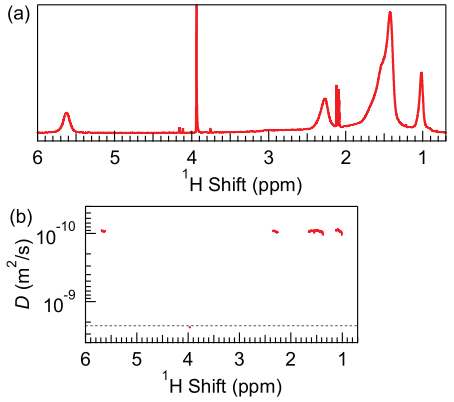

Figure 7. (a) ^{1}H NMR spectrum of OlAc-capped PbS Qdots (7.1 nm) shows only broad resonances. (b) DOSY of a similar suspension (5.5 nm). The small diffusion coefficient confirms that the OlAc ligands are tightly bound to the Qdot surface. The weak signal of the tol-d_8 diffusion coefficient is not shown to avoid a noisy figure but is represented by the dotted line.

TABLE 2. PbS Qdot Size d, Number of OlAc Ligands per Qdot N_{OlAc} and OlAc Ligand Density ρ

d (nm)	N_{OlAc}	ρ (nm^{-2})
5.2	220	2.6
5.5	284	3.0
7.1	554	3.5

A_{meth}/A_{alk} yields the TOP/OlAm ratio.

$$\text{TOP/OlAm} = \frac{2 \times A_{meth}/A_{alk} - 3}{9} \qquad (2)$$

Interestingly, we obtain a ratio of only 0.02:1, that is, within experimental error, TOP is not present. We can explain this apparent contradiction between synthesis and NMR data by considering the PbS Qdot surface composition. A recent determination of the elemental composition of the PbS inorganic core[2,17] showed that the PbS Qdots contain an excess of Pb atoms.[17] In accordance with the nonstoichiometric structural model proposed for PbSe Qdots,[16] the Pb excess is likely located at the Qdot surface. A Pb-rich surface strongly reduces the number of exposed S atoms and thus limits the number of binding sites for TOP.

Capping Exchange to OlAc. Due to the highly dynamic nature of the OlAm ligands and the absence of TOP, the capping can easily be exchanged for OlAc ligands. Figure 7a shows the ^{1}H NMR spectrum of a typical OlAc-capped PbS Qdot suspension (7.1 nm). Next to the CH_2Br_2 resonance at 3.94 ppm, residual toluene at 2.09 ppm, and an unidentified singlet impurity at 2.12 ppm, we only observe broad resonances, with a chemical shift comparable to free OlAc. No sharp resonances arising from free OlAc are discerned. Quantitative ^{1}H NMR measurements on three samples yield an average OlAc coverage of 3.0 ± 0.4 ligands per nm^2 of Qdot surface (Table 2), slightly less than the 4.2 ligands

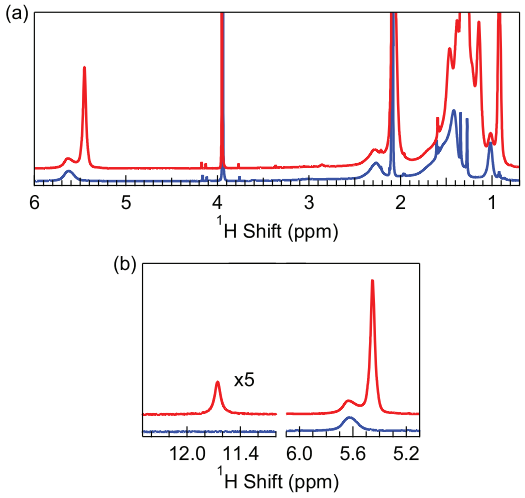

Figure 8. (a) ^{1}H NMR spectrum before (bottom) and after (top) addition of OlAc-d_1. A new set of resonances is present after addition. (b) A small amount of −OH protons is present at 10.57 ppm (spectra 5-fold enhanced). They correspond to the residual protons in the OlAc-d_1 added. The alkene protons are shown for comparison.

per nm^2 observed for PbSe Qdots.[24] The 5.2 nm sample is synthesized without TOP, the other two with TOP. For these samples, quantitative ^{1}H NMR yields an average TOP/OlAc ratio of 0.6%, which confirms the absence of TOP on the PbS Qdot surface. The DOSY spectrum (Figure 7b, measured with δ = 5 ms and Δ = 250 ms) shows that the OlAc ligand diffusion coefficient equals 9.3×10^{-11} m^2/s. The Stokes−Einstein relation yields a hydrodynamic diameter d_H = 8.0 nm, agreeing well with the PbS Qdot core size of 5.5 nm, incremented with the thickness of the OlAc capping layer (1.25 nm, similar to typical values obtained for OlAc-capped PbSe Qdots[24]).

The small diffusion coefficient and broadness of the resonances both demonstrate that the OlAc is tightly bound to the Qdots. However, these data do not reveal the nature of the bond. Two possibilities exist: either a neutral OlAc is adsorbed, yet the adsorption/desorption equilibrium is very close to the adsorbed state (hence no free OlAc is present), or an oleate ion is adsorbed, in which case the ligands cannot be released from the surface without acquiring a proton. To resolve which case applies, we add a 3-fold excess of OlAc with a deuterated carboxylic acid group (OlAc-d_1) to the suspension. The ^{1}H NMR spectrum after OlAc-d_1 addition shows a new set of resonances (Figure 8), attributable to OlAc ligands in a dynamic equilibrium between a free and a bound state. Due to this equilibrium, the new alkene resonance at 5.48 ppm consists of 25% of original OlAc ligands and 75% of the OlAc-d_1 added. However, at 10.57 ppm, we do not observe a corresponding increase of the −OH proton resonance. We observe a ratio of this resonance to the new alkene resonance of 0.11:1. The ratio calculated for neutral OlAc ligands equals (0.25·0.5 + 0.75·0.13):1 = 0.22:1 (the 0.13:1 ratio is due to the 73% yield of the

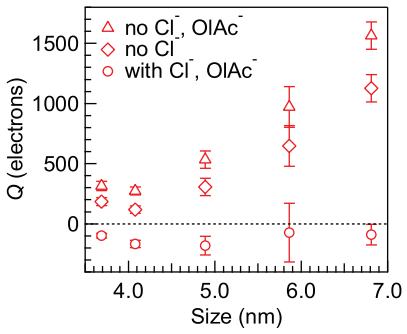

Figure 9. Qdot charge *Q*, expressed as number of electrons, calculated including the layer of surface Cl ions and the OlAc ligands (○). A charge-neutral Qdot is not obtained when neglecting the charge of the Cl ions (◊) and the OlAc ligands (Δ).

OlAc-d_1 prepared; see Methods). More importantly, the experimental value agrees well with the ratio expected for an oleate ligand, which we calculate as (0.75·0.13):1 = 0.10:1. In conclusion, the area under the −OH proton resonance is too small to be arising from neutral OlAc molecules being released from the Qdot surface, which implies that an exchange of an −OD deuterium must take place upon the release of the ligands. This will only occur when they are bound as oleate ligands.

The NMR data now complete our knowledge on the composition of these ligand-exchanged PbS Qdots. With Rutherford backscattering spectroscopy (RBS), we already demonstrated that they consist of a stoichiometric PbS core, surrounded by a surface layer of excess Pb and Cl.[17] Attached to this surface, we now have the oleate ligands, at a density of 3.0 nm^{-2}. This model is supported by a calculation of the Qdot charge balance *Q* (expressed as a number of electrons). Starting from the RBS data for the five PbS Qdot samples studied recently[17] and taking the charge of all constituents into account: Pb^{2+}, S^{2-}, Cl^{1-} and $OlAc^{1-}$, we can write it as (*N* equals the number of atoms or ligands per Qdot, respectively)

$$Q = 2N_{Pb} - 2N_S - N_{Cl} - N_{OlAc} \quad (3)$$

Figure 9 shows that a charge-neutral Qdot is obtained only when, next to the charges of the Pb and S, the charge of the OlAc ligands and Cl ions are both taken into account (○). When either Cl^{1-} (◊) or both Cl^{1-} and $OlAc^{1-}$ (Δ) are neglected, the Qdot charge rapidly deviates from zero with increasing Qdot size. Hence, we conclude that the positive charge of the lead-rich PbS cores is balanced by counter-charges provided by the surface layer of Cl^{1-} ions and oleate ions.

PbS Qdot Stability and Luminescence Properties. Interestingly, for the Cademartiri synthesis, only the original work of Cademartiri *et al.*[2] reports on the PL QY of these Qdots; they found a value of *ca.* 40%. Literature data mostly concern OlAc-capped PbS Qdots synthesized *via* the Hines synthesis. In this case, small Qdots (peak absorption of 1100−1300 nm) typically show a PL QY between 20[1] and 60−80%.[21,22] For larger Qdots (peak

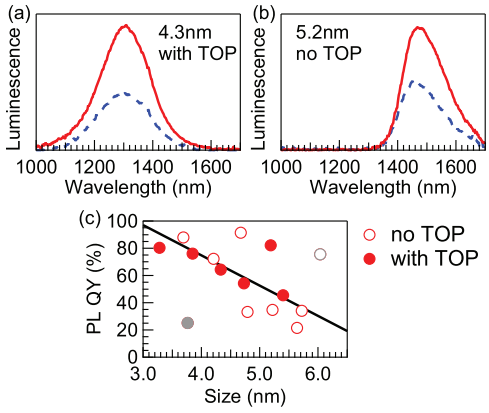

Figure 10. (a,b) Luminescence spectra of OlAm (dashed curve) and OlAc (full curve) capped PbS Qdots. After capping exchange to OlAc, we observe an enhancement in PL QY for both PbS Qdots synthesized with (a) and without (b) TOP, respectively. (c) PL QY for several OlAc-capped PbS Qdots, synthesized either with (●) or without (○) TOP.

absorption of 1300−1600 nm), the PL QY goes down to 25−40%.[22] This is in line with the reduced PL QY observed for large PbSe Qdots.[44] A more in depth study has recently been performed by Semonin *et al.*,[23] where they measured the PL QY for a series of PbSe and PbS Qdot sizes with an integrating sphere. They confirmed the decrease of the PL QY with increasing size and attribute it to a quenching by localized trap states. The resulting monotonic decrease is further modulated by quenching through energy transfer to the ligands' vibrational modes (Förster resonance energy transfer), which yields dips in the PL QY spectrum at wavelengths where the OlAc ligands show a strong absorption.

Here we demonstrate that PbS Qdots prepared with the Cademartiri synthesis also exhibit a high PL QY. First, we investigate the role of the ligands. By measuring the PL spectrum before and after OlAc exchange (Figure 10a,b), we observe that the tightly bound OlAc ligands provide an improved electronic passivation with respect to the highly dynamic OlAm, irrespective of the synthesis employed (either with our without TOP). We typically obtain a 2-fold enhancement of the PL (10 samples measured, 5 synthesized with TOP and 5 without TOP). That TOP does not influence this result is in line with the structural model proposed in the previous section, where it does not play a role in the final PbS Qdot surface composition. Second, the absolute PL QY is determined for a series of OlAc-capped PbS Qdots (3−6 nm, Figure 10c), synthesized both with (●) and without (○) TOP. Again, no appreciable difference is observed between both types. Fitting a line to all data except the outermost two points (gray) shows that, although individual measurements are more scattered than in the report of Semonin *et al.*,[23] the PL QY decreases with size in this range. However, all samples show a high PL QY, varying between 20% for the larger Qdots and 90% for the smaller ones.

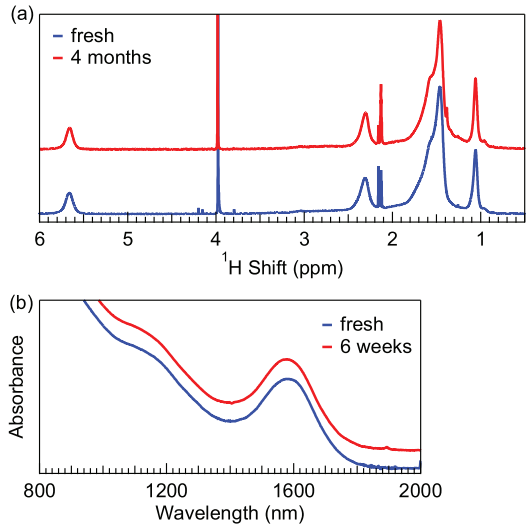

Figure 11. (a) ^{1}H NMR spectra of a fresh PbS Qdot suspension (bottom) and after 4 months (top). (b) Absorbance spectra of a fresh suspension (bottom) and after 6 weeks (top). In both cases, no changes are observed. Spectra are offset for clarity.

Apart from a high luminescence yield, optical stability is also a desirable property if one wishes to apply these Qdots in photonic devices. Using both NMR and absorbance spectroscopy, we demonstrate that OlAc-capped PbS Qdots are stable under ambient conditions. Figure 11a compares the ^{1}H NMR spectrum (5.6 nm Qdots) of a freshly prepared PbS Qdot suspension with the spectrum after 4 months. The absence of any significant changes indicates that the ligands are unperturbed during storage. The stability of the ligand shell suggests that the surface does not oxidize. This in turn results in stable optical properties. Figure 11b shows that the absorbance spectrum of 6.2 nm Qdots is unmodified during storage for 6 weeks. We obtained similar results for smaller Qdots with luminescence spectroscopy.[45] These data strongly contrast with PbSe Qdots.[24−26] Here we observed both a release of OlAc ligands and a subsequent blue shift of the first exciton peak,[24] indicative of a fast oxidation. Interestingly, the results also differ from PbS Qdots prepared *via* the Hines synthesis, where small Qdots are stable, but larger Qdots exhibit a blue shift of the absorbance peak.[27] We hypothesize that the layer of Cl ions,[2,17] which constitutes the main difference between both types PbS Qdots, leads to an enhanced stability of the Qdot surface. This has also been suggested by Cademartiri *et al.*, who observed that PbS Qdot thin films maintain their luminescence even after a plasma treatment.[28] These results emphasize that the synthesis method still can play an important role in the final properties of Qdots with essentially the same PbS core composition.

CONCLUSIONS

By adaptation of the PbS Qdot synthesis described by Cademartiri *et al.*,[2] more specifically by employing TOP during the synthesis, a strongly enlarged range of Qdot sizes can be synthesized. Monodisperse suspensions with an average size between 3 and 10 nm can now be prepared *via* a one-step synthesis. NMR measurements show that the Qdots are capped solely by OlAm ligands, which exhibit a fast dynamical exchange behavior. A lower limit on the exchange rate of 200 s^{-1} is determined from the chemical shift difference between the protons of the α-CH_2 group of free and bound OlAm. As a result of this fast adsorption/desorption, OlAm-capped PbS Qdots may show a poor electronic passivation. However, the fast ligand dynamics enables a facile exchange to OlAc. The OlAc ligands are tightly bound to the Qdot surface as oleate ions, hereby strongly enhancing the luminescence yield to values of up to 90%. The PbS Qdots are air-stable in suspension, offering prospects for operation of PbS Qdot-based photonic devices under ambient conditions.

METHODS

Materials. OlAc (90%) was purchased from Sigma-Aldrich and OlAm (C18-content 80−90%) from Acros Organics. TOP (97%) was purchased from STREM Chemicals. Sulfur (99.999%) and $PbCl_2$ (99.999%) were purchased from Alfa-Aesar. Toluene (99.8%) and EtOH (99.9%, denaturated with 2% methyl ethyl ketone) were purchased from Fiers. Toluene-d_8 (99.96% deuterated) and cyclohexane-d_{12} (99.7% deuterated) were purchased from CortecNet.

PbS Qdot Synthesis. The PbS Qdot synthesis is based on the procedure of Cademartiri *et al.*[2] A stock solution of 0.16 g (5 mmol) of S dissolved in 15 mL of OlAm is prepared by heating the mixture under nitrogen for 30 min at 120 °C. For the synthesis, we typically mix 0.834 g (3 mmol) of $PbCl_2$ and 7.5 mL of OlAm in a three-neck flask. This is degassed for 30 min under nitrogen at 125 °C. Hereafter, we heat up or cool down the $PbCl_2$ solution to the required injection temperature, and we inject 2.25 mL of the OlAm-S stock solution (0.75 mmol of S). The temperature drops approximately 5−10 °C, and the resulting growth temperature is maintained throughout the reaction. After the desired growth time, the reaction is quenched by adding 10 mL of toluene and 15 mL of EtOH. After centrifugation of the suspension and decantation of the supernatant, the Qdots are resuspended in 10 mL of toluene. For the samples studied here, the growth temperature is varied between 80 and 160 °C, although we have observed that the reaction proceeds even at room temperature. To monitor the Qdot growth, aliquots are taken at times ranging from 20 s up to 2.5 h.

To investigate the effect of TOP on the synthesis, we repeat all syntheses with 170 μL (375 μmol, half of the amount of S) of TOP added to the 2.25 mL of OlAm-S. TOP is added at room temperature, and after stirring, the solution has a lighter color. As TOPS is colorless, while OlAm-S is dark red, this is taken as evidence that half of the OlAm-S is converted to TOPS.

Qdot Characterization. In a previous report, we have shown with transmission electron microscopy (TEM) that the PbS Qdots are spherical and of uniform size.[17] Relating the TEM diameter to the Qdot band gap E_0 (eV), measured with absorbance spectroscopy, we have constructed a sizing curve, which enables to determine the size d (nm) directly from the spectral

position of the first absorption peak.

$$E_0 = 0.41 + \frac{1}{0.0252d^2 + 0.283d} \quad (4)$$

In addition, the Qdot molar extinction coefficient ε was determined. Its value at 400 nm ε_{400} is used to calculate the Qdot concentration c_0 directly from the absorbance at 400 nm A_{400} using Beer's law: $A = \varepsilon.c_0.L$ (L is the sample length).

$$\varepsilon_{400} = 0.0234d^3 \text{ cm}^{-1}/\mu\text{M} \quad (5)$$

Samples for absorbance spectroscopy are prepared by drying a known amount of Qdots and suspending them in tetrachloroethylene (C_2Cl_4).

To determine the synthesis yield, aliquots are weighed (mass, M_{aliq}) in order to calculate the amount taken from the synthesis (total mass of the synthesis, M_{tot}). After workup, the Qdots are suspended in a known volume V_{abs} and c_0 is determined. Taking the PbS lattice constant a and Pb/S ratio R of the Qdots into account[17] ($R = 1.26$), the number of S atoms per Qdot is known and the synthesis yield Y_S, related to the amount of sulfur N_S injected, can be calculated.

$$Y_S = \frac{M_{tot}}{M_{aliq}} V_{abs} \frac{A_{400}}{\varepsilon_{400} L} \frac{4\pi}{3} \left(\frac{d}{a}\right)^3 \frac{1}{1+R} \frac{1}{N_S} \quad (6)$$

Ligand Exchange. After synthesis, we observed that the Qdots cannot be precipitated and resuspended more than once. A turbid suspension results, clearly indicating a loss of ligands and subsequent PbS Qdot clustering. The OlAm ligands can however easily be replaced. An exchange to OlAc is typically performed by adding OlAc to a toluene suspension of PbS Qdots in a ratio of 1.5:10 OlAc/toluene. After precipitation with EtOH and centrifugation, the Qdots are resuspended in toluene and the exchange is repeated. Finally, the Qdots are precipitated one more time with EtOH to remove any excess OlAc. After capping exchange, the Qdots can be precipitated several times, suggesting a successful exchange of the capping to OlAc.

Ligand Characterization. The ligands are investigated with solution NMR. Samples are prepared by drying a known amount of PbS Qdots in toluene under a strong nitrogen flow, followed by resuspension in 750 μL of tol-d_8. All NMR measurements are performed at 295 K. The ligand composition and dynamics are established by means of ^{1}H spectra, ^{1}H−^{13}C HSQC spectroscopy, NOESY, and DOSY measurements, performed with a Bruker DRX 500 equipped with a TXI Z-gradient probe, and operating at ^{1}H and ^{13}C frequencies of 500.13 and 125.76 MHz, respectively. For an adequate sampling of the slowest diffusing species, δ and Δ are optimized for each DOSY. The signal decay as a function of gradient strength G is fitted with the Stejskal−Tanner equation,[46] which yields the diffusion coefficient D. When plotting D as a function of the ^{1}H chemical shift, we obtain a 2D DOSY spectrum. For a more in depth discussion on the use of DOSY on colloidal Qdot suspensions, we refer to our previous work.[24]

We determine the ligand grafting density by adding a known amount of dibromomethane (CH_2Br_2, 1−2 μL) as a concentration standard to the NMR samples and measuring the ^{1}H NMR spectra under conditions of full T_1 relaxation (relaxation delay, $d_1 = 45$ s). By comparing the area under the ligand resonances to the area under the CH_2Br_2 resonance, the concentration of ligands is determined. From the known concentration of PbS Qdots in the NMR sample, we then derive the number of ligands per Qdot.

OlAc-d_1 is prepared following a previously published procedure,[47] resulting in a 0.66 M solution of OlAc-d_1 in cyclohexane-d_{12}. Quantitative ^{1}H NMR shows that the ratio of −OH protons to alkene protons equals 0.13:1, that is, 73% of the OlAc is converted into OlAc-d_1. This is sufficient for the current investigation. Next, 30 μL of this solution is added to a PbS Qdot suspension (PbS concentration of 77 μM) to further investigate the nature of the ligand−Qdot bond.

Luminescence Measurements. The steady-state photoluminescence is measured using an Edinburgh Instruments FS920 PL setup. Samples are prepared by drying a known amount of PbS Qdots, followed by resuspension in 4 mL of C_2Cl_4. The absorbance at the band gap is kept below 0.05 cm^{-1} to avoid reabsorption of the emitted light. The samples are excited at 400 nm using a 500 W xenon lamp, coupled to a monochromator. The emitted light is detected using a liquid N_2 cooled Ge detector, coupled to a monochromator. The Ge detector limits the wavelength range to *ca.* 1700 nm, and as such, we are only able to determine the PL spectrum of Qdots up to 6 nm. The emission slits are set to a wavelength resolution of 3 nm. The stability of the excitation lamp and setup is checked by measuring the same sample at the beginning and at the end of the measurements. The difference between both spectra is less than 1%. The emitted photon flux F_λ at a given wavelength λ (nm) is corrected for detector and grating efficiency and converted to an flux F_{eV} on an energy scale (eV):

$$F_{eV} = F_\lambda \frac{\lambda^2}{1239.85} \quad (7)$$

The resulting F_{eV} spectra are fitted using a sum of two Gaussian curves. The total emitted photon flux Φ_{Qdot} equals the area under these curves.

For one Qdot sample (the reference), we determine the PL QY (QY_{ref}) directly using a calibrated integrating sphere.[48] For the other samples, the PL QY (QY_{sample}) is calculated relative to this reference sample, taking their respective sample transmittance T into account:

$$QY_{sample} = QY_{ref} \frac{\Phi_{Qdot,sample}}{\Phi_{Qdot,ref}} \frac{1 - T_{ref}}{1 - T_{sample}} \quad (8)$$

Acknowledgment. I.M. is a postdoctoral researcher with the FWO-Vlaanderen. This project is funded by the EU Seventh Framework Program (EU-FP7 ITN Herodot), the FWO-Vlaanderen (G.0.144.08.N.10) and Ghent University (NB Photonics). D. Poelman (Department of Solid State Sciences, Ghent University) is acknowledged for the use of the luminescence setup. S. Flamée is acknowledged for measuring the TEM images.

REFERENCES AND NOTES

1. Hines, M. A.; Scholes, G. D. Colloidal PbS Nanocrystals with Size-Tunable Near-Infrared Emission: Observation of Post-Synthesis Self-Narrowing of the Particle Size Distribution. *Adv. Mater.* **2003,** *15*, 1844–1849.
2. Cademartiri, L.; Bertolotti, J.; Sapienza, R.; Wiersma, D. S.; von Freymann, G.; Ozin, G. A. Multigram Scale, Solventless, and Diffusion-Controlled Route to Highly Monodisperse PbS Nanocrystals. *J. Phys. Chem. B* **2006,** *110*, 671–673.
3. Murray, C. B.; Sun, S. H.; Gaschler, W.; Doyle, H.; Betley, T. A.; Kagan, C. R. Colloidal Synthesis of Nanocrystals and Nanocrystal Superlattices. *IBM J. Res. Dev.* **2001,** *45*, 47–56.
4. Murphy, J. E.; Beard, M. C.; Norman, A. G.; Ahrenkiel, S. P.; Johnson, J. C.; Yu, P.; Micic, O. I.; Ellingson, R. J.; Nozik, A. J. PbTe Colloidal Nanocrystals: Synthesis, Characterization, and Multiple Exciton Generation. *J. Am. Chem. Soc.* **2006,** *128*, 3241–3247.
5. Urban, J. J.; Talapin, D. V.; Shevchenko, E. V.; Murray, C. B. Self-Assembly of PbTe Quantum Dots into Nanocrystal Superlattices and Glassy Films. *J. Am. Chem. Soc.* **2006,** *128*, 3248–3255.
6. Urban, J. J.; Talapin, D. V.; Shevchenko, E. V.; Kagan, C. R.; Murray, C. B. Synergism in Binary Nanocrystal Superlattices Leads to Enhanced p-Type Conductivity in Self-Assembled PbTe/Ag_2Te Thin Films. *Nat. Mater.* **2007,** *6*, 115–121.
7. Bakueva, L.; Musikhin, S.; Hines, M. A.; Chang, T. W. F.; Tzolov, M.; Scholes, G. D.; Sargent, E. H. Size-Tunable Infrared (1000−1600 nm) Electroluminescence from PbS Quantum-Dot Nanocrystals in a Semiconducting Polymer. *Appl. Phys. Lett.* **2003,** *82*, 2895–2897.
8. Konstantatos, G.; Huang, C. J.; Levina, L.; Lu, Z. H.; Sargent, E. H. Efficient Infrared Electro-luminescent Devices Using Solution-Processed Colloidal Quantum Dots. *Adv. Funct. Mater.* **2005,** *15*, 1865–1869.

9. Hoogland, S.; Sukhovatkin, V.; Howard, I.; Cauchi, S.; Levina, L.; Sargent, E. H. A Solution- Processed 1.53 μm Quantum Dot Laser with Temperature-Invariant Emission Wavelength. *Opt. Express* **2006,** *14*, 3273–3281.
10. Luther, J. M.; Law, M.; Beard, M. C.; Song, Q.; Reese, M. O.; Ellingson, R. J.; Nozik, A. J. Schottky Solar Cells Based on Colloidal Nanocrystal Films. *Nano Lett.* **2008,** *8*, 3488–3492.
11. Sargent, E. H. Infrared Photovoltaics Made by Solution Processing. *Nat. Photonics* **2009,** *3*, 325–331.
12. McDonald, S. A.; Konstantatos, G.; Zhang, S. G.; Cyr, P. W.; Klem, E. J. D.; Levina, L.; Sargent, E. H. Solution-Processed PbS Quantum Dot Infrared Photodetectors and Photovoltaics. *Nat. Mater.* **2005,** *4*, 138–142.
13. Rauch, T.; Boberl, M.; Tedde, S. F.; Furst, J.; Kovalenko, M. V.; Hesser, G. N.; Lemmer, U.; Heiss, W.; Hayden, O. Near-Infrared Imaging with Quantum-Dot-Sensitized Organic Photodiodes. *Nat. Photonics* **2009,** *3*, 332–336.
14. Tang, J.; Wang, X. H.; Brzozowski, L.; Barkhouse, D. A. R.; Debnath, R.; Levina, L.; Sargent, E. H. Schottky Quantum Dot Solar Cells Stable in Air under Solar Illumination. *Adv. Mater.* **2010,** *22*, 1398–1402.
15. Ma, W.; Luther, J. M.; Zheng, H. M.; Wu, Y.; Alivisatos, A. P. Photovoltaic Devices Employing Ternary PbS_xSe_{1-x} Nanocrystals. *Nano Lett.* **2009,** *9*, 1699–1703.
16. Moreels, I.; Lambert, K.; De Muynck, D.; Vanhaecke, F.; Poelman, D.; Martins, J. C.; Allan, G.; Hens, Z. Composition and Size-Dependent Extinction Coefficient of Colloidal PbSe Quantum Dots. *Chem. Mater.* **2007,** *19*, 6101–6106.
17. Moreels, I.; Lambert, K.; Smeets, D.; De Muynck, D.; Nollet, T.; Martins, J. C.; Vanhaecke, F.; Vantomme, A.; Delerue, C.; Allan, G..; *et al.* Size-Dependent Optical Properties of Colloidal PbS Quantum Dots. *ACS Nano* **2009,** *3*, 3023–3030.
18. Du, H.; Chen, C. L.; Krishnan, R.; Krauss, T. D.; Harbold, J. M.; Wise, F. W.; Thomas, M. G.; Silcox, J. Optical Properties of Colloidal PbSe Nanocrystals. *Nano Lett.* **2002,** *2*, 1321–1324.
19. Wehrenberg, B. L.; Wang, C. J.; Guyot-Sionnest, P. Interband and Intraband Optical Studies of PbSe Colloidal Quantum Dots. *J. Phys. Chem. B* **2002,** *106*, 10634–10640.
20. Brumer, M.; Sirota, M.; Kigel, A.; Sashchiuk, A.; Galun, E.; Burshtein, Z.; Lifshitz, E. Nanocrystals of PbSe Core, PbSe/PbS, and PbSe/$PbSe_xS_{1-x}$ Core/Shell as Saturable Absorbers in Passively Q-Switched Near-Infrared Lasers. *Appl. Opt.* **2006,** *45*, 7488–7497.
21. Lin, W.; Fritz, K.; Guerin, G.; Bardajee, G. R.; Hinds, S.; Sukhovatkin, V.; Sargent, E. H.; Scholes, G. D.; Winnik, M. A. Highly Luminescent Lead Sulfide Nanocrystals in Organic Solvents and Water through Ligand Exchange with Poly(acrylic acid). *Langmuir* **2008,** *24*, 8215–8219.
22. Abel, K. A.; Shan, J. N.; Boyer, J. C.; Harris, F.; van Veggel, F. C. J. M. Highly Photoluminescent PbS Nanocrystals: The Beneficial Effect of Trioctylphosphine. *Chem. Mater.* **2008,** *20*, 3794–3796.
23. Semonin, O. E.; Johnson, J. C.; Luther, J. M.; Midgett, A. G.; Nozik, A. J.; Beard, M. C. Absolute Photoluminescence Quantum Yields of IR-26 Dye, PbS, and PbSe Quantum Dots. *J. Phys. Chem. Lett.* **2010,** *1*, 2445–2450.
24. Moreels, I.; Fritzinger, B.; Martins, J. C.; Hens, Z. Surface Chemistry of Colloidal PbSe Nanocrystals. *J. Am. Chem. Soc.* **2008,** *130*, 15081–15086.
25. Dai, Q. Q.; Wang, Y. N.; Zhang, Y.; Li, X. B.; Li, R. W.; Zou, B.; Seo, J.; Wang, Y. D.; Liu, M. H.; Yu, W. W. Stability Study of PbSe Semiconductor Nanocrystals over Concentration, Size, Atmosphere, and Light Exposure. *Langmuir* **2009,** *25*, 12320–12324.
26. Sykora, M.; Koposov, A. Y.; McGuire, J. A.; Schulze, R. K.; Tretiak, O.; Pietryga, J. M.; Klimov, V. I. Effect of Air Exposure on Surface Properties, Electronic Structure, and Carrier Relaxation in PbSe Nanocrystals. *ACS Nano* **2010,** *4*, 2021–2034.
27. Tang, J.; Brzozowski, L.; Barkhouse, D. A. R.; Wang, X. H. Debnath, R.; Wolowiec, R.; Palmiano, E.; Levina, L.; Pattantyus-Abraham, A. G.; Jamakosmanovic, D..; *et al.* Quantum Dot Photovoltaics in the Extreme Quantum Confinement Regime: The Surface-Chemical Origins of Exceptional Air- and Light-Stability. *ACS Nano* **2010,** *4*, 869–878.
28. Cademartiri, L.; von Freymann, G.; Arsenault, A. C.; Bertolotti, J.; Wiersma, D. S.; Kitaev, V.; Ozin, G. A. Nanocrystals as Precursors for Flexible Functional Films. *Small* **2005,** *1*, 1184–1187.
29. Bullen, C. R.; Mulvaney, P. Nucleation and Growth Kinetics of CdSe Nanocrystals in Octadecene. *Nano Lett.* **2004,** *4*, 2303–2307.
30. Rempel, J. Y.; Bawendi, M. G.; Jensen, K. F. Insights into the Kinetics of Semiconductor Nanocrystal Nucleation and Growth. *J. Am. Chem. Soc.* **2009,** *131*, 4479–4489.
31. Zheng, H.; Smith, R. K.; Wook Jun, Y.; Kisielowski, C.; Dahmen, U.; Alivisatos, A. P. Observation of Single Colloidal Platinum Nanocrystal Growth Trajectories. *Science* **2009,** *324*, 1309–1312.
32. Peng, X. G.; Wickham, J.; Alivisatos, A. P. Kinetics of II–VI and III–V Colloidal Semiconductor Nanocrystal Growth: "Focusing" of Size Distributions. *J. Am. Chem. Soc.* **1998,** *120*, 5343–5344.
33. Talapin, D. V.; Rogach, A. L.; Haase, M.; Weller, H. Evolution of an Ensemble of Nanoparticles in a Colloidal Solution: Theoretical Study. *J. Phys. Chem. B* **2001,** *105*, 12278–12285.
34. Evans, C. M.; Evans, M. E.; Krauss, T. D. Mysteries of TOPSe Revealed: Insights into Quantum Dot Nucleation. *J. Am. Chem. Soc.* **2010,** *132*, 10973–10975.
35. Bullen, C.; Mulvaney, P. The Effects of Chemisorption on the Luminescence of CdSe Quantum Dots. *Langmuir* **2006,** *22*, 3007–3013.
36. Pradhan, N.; Reifsnyder, D.; Xie, R. G.; Aldana, J.; Peng, X. G. Surface Ligand Dynamics in Growth of Nanocrystals. *J. Am. Chem. Soc.* **2007,** *129*, 9500–9509.
37. Ji, X. H.; Copenhaver, D.; Sichmeller, C.; Peng, X. G. Ligand Bonding and Dynamics on Colloidal Nanocrystals at Room Temperature: The Case of Alkylamines on CdSe Nanocrystals. *J. Am. Chem. Soc.* **2008,** *130*, 5726–5735.
38. Koole, R.; Schapotschnikow, P.; de Mello Donega, C.; Vlugt, T. J. H.; Meijerink, A. Time- Dependent Photoluminescence Spectroscopy as a Tool To Measure the Ligand Exchange Kinetics on a Quantum Dot Surface. *ACS Nano* **2008,** *2*, 1703–1714.
39. Fritzinger, B.; Moreels, I.; Lommens, P.; Koole, R.; Hens, Z.; Martins, J. C. *In Situ* Observation of Rapid Ligand Exchange in Colloidal Nanocrystal Suspensions Using Transfer NOE Nuclear Magnetic Resonance Spectroscopy. *J. Am. Chem. Soc.* **2009,** *131*, 3024–3032.
40. Hens, Z.; Moreels, I.; Martins, J. C. *In Situ* H-1 NMR Study on the Trioctylphosphine Oxide Capping of Colloidal InP Nanocrystals. *ChemPhysChem* **2005,** *6*, 2578–2584.
41. Moreels, I.; Martins, J. C.; Hens, Z. Ligand Adsorption/Desorption on Sterically Stabilized InP Colloidal Nanocrystals: Observation and Thermodynamic Analysis. *ChemPhysChem* **2006,** *7*, 1028–1031.
42. Clore, G. M.; Gronenborn, A. M. Theory and Applications of the Transferred Nuclear Overhauser Effect to the Study of the Conformations of Small Ligands Bound to Proteins. *J. Magn. Reson.* **1982,** *48*, 402–417.
43. Bain, A. D. Chemical Exchange in NMR. *Prog. Nucl. Magn. Reson. Spectrosc.* **2003,** *43*, 63–103.
44. Pietryga, J. M.; Schaller, R. D.; Werder, D.; Stewart, M. H.; Klimov, V. I.; Hollingsworth, J. A. Pushing the Band Gap Envelope: Mid-Infrared Emitting Colloidal PbSe Quantum Dots. *J. Am. Chem. Soc.* **2004,** *126*, 11752–11753.
45. Justo, Y.; Moreels, I.; Lambert, K.; Hens, Z. Langmuir–Blodgett Monolayers of Colloidal Lead Chalcogenide Quantum Dots: Morphology and Photoluminescence. *Nanotechnology* **2010,** *21*, 295606.
46. Wu, D. H.; Chen, A. D.; Johnson, C. S. An Improved Diffusion-Ordered Spectroscopy Experiment Incorporating Bipolar-Gradient Pulses. *J. Magn. Reson., Ser. A* **1995,** *115*, 260–264.
47. Fritzinger, B.; Capek, R.; Lambert, K.; Martins, J. C.; Hens, Z. Utilizing Self-Exchange To Address the Binding of Carboxylic Acid Ligands to CdSe Quantum Dots. *J. Am. Chem. Soc.* **2010,** *132*, 10195–10201.
48. de Mello, J. C.; Wittmann, H. F.; Friend, R. H. An Improved Experimental Determination of External Photoluminescence Quantum Efficiency. *Adv. Mater.* **1997,** *9*, 230–232.